

F. Lunkeit · K. Fraedrich · S. E. Bauer

Storm tracks in a warmer climate: sensitivity studies with a simplified global circulation model

Received: 17 December 1996 / Accepted: 14 May 1998

Abstract A simplified global circulation model is used to analyse a greenhouse warming experiment simulated by a comprehensive general circulation model. The given GCM scenario and control climates are assimilated by the simplified model using a dynamical relaxation technique. Two sets of sensitivity experiments investigate the influence of upper and lower tropospheric changes in baroclinicity on the Northern Hemisphere winter storm tracks. The results show that the three-dimensional structure of both the background flow and the changes in baroclinicity are important for the behaviour of mid-latitude eddy activity in relation to modifications of the baroclinicity. In general, the mid-latitude eddy activity is more sensitive to lower than to upper level changes in baroclinicity. The results further suggest that the simulated storm track changes in the GCM scenario are dominated by local modes of baroclinic instability.

1 Introduction

An increasing number of research groups have investigated the global warming problem using comprehensive general circulation models (GCM) of the coupled atmosphere-ocean climate system. These models provide reasonable and consistent evidence of possible climate change. Among the many aspects related to global warming, the potential effect on the mid-latitude eddies and the associated storm tracks is fundamental. In particular, the variability of the North Atlantic storm track is important, because changes in this area will lead to perceptible consequences on strong

weather systems over Europe (von Storch et al. 1993). GCM studies which attempt to address this problem do not provide an unequivocal confirmation of the changes that are expected in the storm track (e.g. Hall et al. 1994; Siegmund 1990a,b; Stephenson and Held 1993; Lunkeit et al. 1996b). This is partly due to uncertainties in the simulated time-mean response, which is a result of deficiencies in the model and the chosen forcing (e.g. the amount of greenhouse gas increase). The time-mean climate change as simulated by all GCMs suggests that there are counteracting effects on the transients. Due to the highly nonlinear relationship between the time-mean circulation and the transient eddies, small deviations of the time-mean response could result in large differences in the eddy activity. Therefore, sensitivity studies are needed to assess the robustness of the GCM simulations to perturbations. For example, the relationship between changes of the time-mean flow and the eddy activity needs to be explored. However, to separate individual processes in a full GCM is complicated and, in addition, sensitivity studies with comprehensive GCMs are limited by the huge demand of computer power.

Here we use an alternative approach to analyse GCM results. A simplified global circulation model (the portable university model of the atmosphere; PUMA) is used to construct a GCM climate and to perform a set of sensitivity experiments. The model is simplified in such a way that the particular point of interest, namely the dynamical aspects of eddy mean flow interaction, can be analysed systematically. The model is based on the primitive equations, but does not involve any of the complex parametrisations commonly used in GCMs, except Newtonian cooling and Rayleigh friction; there are also no moist processes or any variations of surface properties. Because of these simplifications, PUMA has the advantage that only a small amount of computing time is required and the model is easy to handle. In order to simulate the characteristics of the time averaged atmospheric circulation

F. Lunkeit · K. Fraedrich (✉) · S. E. Bauer
Meteorologisches Institut, Universität Hamburg,
Bundesstraße 55, D-20146 Hamburg, Germany
E-mail: fraedrich@dkrz.de

with PUMA, a forcing is needed that substitutes the most important effects induced by the disregarded physical parametrisations. In the present work we describe a technique to assimilate a forcing field, which allows the simple model to simulate a climate state sufficiently close to that predicted by more complex GCMs. By developing a suitable assimilation approach and employing it, sensitivity experiments can be easily realised by varying these forcing fields.

This study is focused on the relation between changes in the time-mean flow and the eddy activity. The motivation is taken from the observation that most greenhouse warming simulations reveal an increase in the upper troposphere equator to pole temperature gradient and a decreasing lower tropospheric gradient. But, considering classical baroclinic instability theory (Eady 1949, Charney 1947, Phillips 1951, etc.) these opposing changes in the upper and lower troposphere should have counteracting effects on the eddies. Held and O'Brien (1992) and Pavan (1996) have investigated this problem with a multi-layer quasi-geostrophic β -channel model, studying the influence of the vertical structure of the basic state temperature gradients on the baroclinic eddy fluxes. Both analyses conclude that the low-level temperature gradient has a stronger influence on the baroclinic eddy fluxes than the upper-level gradient. However, their studies do not consider that the observed eddy activity has a non-uniform spatial distribution. In the Northern Hemisphere, for example, the high frequency variability is localised in the North Atlantic and North Pacific storm track (Blackmon 1976; Blackmon et al. 1977). Therefore, it is necessary to account for the three-dimensional structure.

A relationship between the storm track variability and the baroclinicity of the time-mean flow, measured by the maximum Eady growth rate, has been demonstrated in observational data by Valdes and Hoskins (1989). Consistent results regarding the storm track – baroclinicity relationship were also found in GCM scenarios by Hall et al. (1994) and Lunkeit et al. (1996b). However, a separation of the opposing effects in the upper and lower troposphere, is hardly possible in the GCM data set.

In the investigations reported here PUMA is used as a tool to analyse the time averaged winter (DJF) climate performed by a greenhouse warming experiment of the GCM, ECHAM2/OPYC (Lunkeit et al. 1996a,b). Sensitivity studies are being made with the PUMA model to separate the influence of the upper and lower-level baroclinicity changes on the storm tracks predicted by the ECHAM2/OPYC global warming simulations, taking into account the three-dimensional structure of the circulation.

The work is outlined as follows: after a brief description of the PUMA model (Sect. 2), the assimilation technique to calculate a suitable forcing field for a given climate is described in Sect. 3. Section 4 presents the

global warming experiment with PUMA and shows the results compared to the ECHAM2/OPYC simulation. The sensitivity studies are discussed in Sect. 5, which include (a) zonal mean sensitivity experiments, (b) three-dimensional sensitivity experiments and (c) experiments on the robustness of the sensitivity experiments with respect to orography. A summary and the conclusions (Sect. 6) close the work.

2 The simple model

The PUMA model is a modification (carried out at the University of Hamburg) of the simplified global circulation model which was introduced by Hoskins and Simmons (1975) and James and Gray (1986). PUMA has been developed to be run on several different computer platforms and to provide an easily applicable global circulation model compatible to ECHAM for scientific and educational purposes at universities. Former versions of PUMA have been mainly used for idealised studies. For example, James and Gray (1986), James and James (1992) and James et al. (1994) run the model using a forcing of a zonally symmetric equator to pole temperature gradient, to study the influence of surface friction on the circulation of a baroclinic atmosphere and ultra-low-frequency variability; the baroclinic adjustment in the context of a zonally varying flow are studied by Mole and James (1990) and Frisius et al. (1998) simulate an idealised storm track by embedding a dipole structure into a zonally symmetric forcing field.

The model is based on the primitive equations which are solved using a spectral representation of fields in the horizontal with triangular truncation and finite differences on equally spaced σ levels in the vertical (T21 truncation and ten levels in the present study). Unresolved processes are parametrised by internal horizontal hyperdiffusion ($\sim \nabla^8$) applied to vorticity, divergence and temperature representing the effects of subgrid scale eddies. Rayleigh friction acting on vorticity and divergence provide for the large-scale dissipation; it is confined to the three lowest model layers and leads to an e-folding decay of the velocities on a time scale $\tau_D = 1, 5, 10$ days at the model layers $\sigma = 0.95, 0.85, 0.75$, respectively. To keep the model as simple as possible variations of surface properties, such as roughness, are not considered. Orography is not included (see Sect. 5c). All processes contributing to the diabatic heating (cooling) of the atmosphere are attributed to the Newtonian relaxation term on the right hand side of the thermodynamic equation:

$$\frac{\partial T'}{\partial t} + \mathcal{L}(T) + \mathcal{N}(T) = \frac{(T_E - T)}{\tau_E} \quad (1)$$

where T describes the temperature, T' the anomaly to a reference temperature on σ levels, $\bar{T}(\sigma)$, defined by $T = \bar{T}(\sigma) + T'$; $\mathcal{N}(T)$ and $\mathcal{L}(T)$ are the nonlinear and linear terms.

The Newtonian formulation may be interpreted as an idealised radiative-convective heating with T_E being a fictive equilibrium temperature. In our experiments the model is relaxed towards the restoration temperature field T_E , using a time scale $\tau_E = 30$ days at all levels.

As the Newtonian cooling term represents the only forcing of the model, the structure of the restoration temperature field T_E determines the simulated mean circulation. A linear relationship between the restoration temperature field T_E and the time-mean temperature field \bar{T} of the model cannot be expected, because contributions by the nonlinear terms $\mathcal{N}(T)$ are large. Analysing climate sensitivity by simple GCMs like PUMA, requires a suitable restoration temperature field T_E which is associated with the prescribed target time-mean temperature field, T_{target} , of the climate to be studied. This leads to a data assimilation technique developed in the following section.

3 Assimilation technique

The aim of the present study is to analyse climate states obtained from GCM simulations. As pointed out in the previous section, the PUMA circulation is driven by Newtonian relaxation of the model temperature T towards a restoration temperature field T_E , defined in the thermodynamic equation (Eq. 1). Therefore, in order to simulate a given climate, it is necessary to assimilate a restoration temperature field T_E such that the time-mean circulation of the simplified PUMA model corresponds to the GCM climate, that is, the target state. To assimilate a suitable restoration temperature field T_E we note the following points:

1. T_{target} is the time averaged three-dimensional temperature distribution taken from the target state, which is the temperature (observed or modelled) to be assimilated by PUMA preceding the numerical experiments
2. Due to the temperature advection the restoration temperature T_E does not match the climatologically averaged temperature \bar{T} of the model: in the time mean, the Newtonian cooling term (representing the total diabatic heating) balances the a priori unknown temperature advection. Considering, for example, a total diabatic heating of the order of 5 K/day, a large temperature contrast between T_E and \bar{T} (150 K) is to be expected if the relaxation time scale ($\tau_E \sim 30$ day) is large. Therefore, replacing T_E by the target temperature T_{target} is not expected to be a successful representation of the forcing of the model.
3. An iterative procedure is introduced to estimate the adequate restoration temperature distribution T_E from T_{target} by modifying the actual restoration temperature field iteratively, $T_E(n)$, $T_E(n+1)$, etc., by the difference between target and model temperature at each time step during the PUMA assimilation run:

$$T_E(n+1) = T_E(n) + \frac{(T_{target} - T)}{\tau_A} \quad (2)$$

$T_E(n)$ denotes the restoration field (at the n -th iteration timestep), T_{target} is the target temperature to be assimilated by the PUMA model and T is the PUMA model temperature. A time scale of the assimilation is introduced by τ_A (a value of $\tau_A = 100$ days is used). For the first iteration the model is forced by the target temperature, $T_E(n=1) = T_{target}$. After a transition phase, a quasi-stationary restoration field $T_E(n)$ develops.

4. Two ways to define the restoration temperature T_E in the Newtonian cooling term are tested: (a) the quasi-stationary restoration field is averaged over the last decades of the PUMA assimilation run to obtain a fixed restoration temperature $T_E = \bar{T}_E(n)$. (b) The update procedure for T_E is continued in order to parametrise low frequency variability of the ‘external’ forcing T_E/τ_E (e.g. fluctuations of the sea surface temperature) which results from negative feedback mechanisms. Both methods appear to be suitable to reproduce the target climate. The continuous update gives slightly better results, which might be a consequence of the large low frequency component being present in the target climate taken from a coupled GCM. Therefore, the continuous update method (b) is chosen for the studies presented here.

The basic idea of the assimilation technique can be illustrated as follows. Consider a model which consists only of a thermodynamic equation (Eq. 1)

$$\frac{\partial T}{\partial t} = \frac{(T_E - T)}{\tau_E} - \mathcal{L}(T) - \mathcal{N}(T) \quad (3)$$

and the additional T_E -update described (Eq. 2)

$$\frac{\partial T_E}{\partial t} = \frac{(T_{target} - T)}{\tau_A} \quad (4)$$

For this model, the climatological mean of the quasi-stationary state ($\frac{\partial T}{\partial t} = \frac{\partial T_E}{\partial t} = 0$) is given by $\bar{T} = T_{target}$ as desired.

Assuming $\mathcal{L}(T)$ and $\mathcal{N}(T)$ in the temperature equation to be constant and independent from T , the stationary solution $T = T_{target}$ is approached via a damped oscillation:

$$\frac{\partial^2 T}{\partial t^2} + \frac{1}{\tau_E} \frac{\partial T}{\partial t} + \frac{T}{\tau_E \tau_A} = \frac{T_{target}}{\tau_E \tau_A} \quad (5)$$

with $\tau_A = 4\tau_E$ being the aperiodic limit.

This assimilation technique is now adopted to determine a suitable forcing to represent a climate state taken from a coupled GCM climate. Simulations and sensitivity experiments discussed in the following section are based on two assimilated GCM climate states: control and $3 \times \text{CO}_2$ -scenario.

4 The global warming experiment

PUMA sensitivity experiments are used to analyse GCM global warming simulations. Two target data sets are defined by simulations based on a global coupled atmosphere-ocean general circulation model (ECHAM2/OPYC; Lunkeit et al. 1996a,b): the last decade of a 100 years transient greenhouse warming experiment (IPCC Scenario A) and the corresponding decade of a control run (210 y present-day climate). The ECHAM2/OPYC model consists of the spectral atmospheric general circulation model ECHAM2 (Roeckner et al. 1992) using a T21 resolution with 19 hybrid levels in the vertical, coupled with the oceanic general circulation model OPYC (Oberhuber 1993a,b); the control and the scenario simulations are described in detail by Lunkeit et al. (1996a,b). The Northern Hemisphere winter (DJF) climate of the last decade of the scenario simulation and the corresponding decade of the control run define the two target climates for the PUMA experiments. In this period the carbon dioxide concentration in the scenario simulation is approximately three times that of the control run. To ensure the reliability of the sensitivity experiments, the PUMA model should be able to reproduce both the control climate and the climate change scenario simulation by the GCM.

Suitable restoration temperatures T_E for the PUMA experiments are determined, as outlined in the previous Sect. 3, using the time-mean temperature fields of the GCM climatologies as target temperatures. These temperatures are extracted on ten pressure surfaces corresponding to the vertical resolution of PUMA. As PUMA does not include orography, the target temperature T_{target} is adapted to the corresponding σ -levels by assuming a fixed surface pressure of 1013 hPa. The extrapolation to pressure surfaces below the ECHAM surface pressure is carried out by considering the lapse rate of the standard atmosphere.

The PUMA-control (CTL) and scenario (SCE) simulations are two 100 y runs (one year consists of 12 permanent winter months), where the T_E -field is updated continuously (e.g. Sect. 3). After an initial transition phase of about 30 y a quasi-stationary T_E -field is obtained. The time average over the last decade

of the 100 y CTL and SCE simulations, respectively, are subjected to further analysis.

Figure 1a shows the time averaged heating rate, $(T_E - T)/\tau_E$ in K/day on 950 hPa, which defines the

Newtonian cooling of the CTL run. There is a general cooling over the continents and a warming over the ocean, which is strongest over the warm currents of the western Atlantic and Pacific oceans.

Except for deviations in the Tibetan Plateau, this heating distribution is comparable with the diabatic heating found by Valdes and Hoskins (1989; Fig. 2a) representing the complex interaction between several forcing effects contributed by the diabatic heating due to latent heat release, radiation and surface fluxes, orography and eddy fluxes. The strong positive heating values in the Tibetan region may be a consequence of the missing orography in PUMA. Likewise, at other regions with high orography the PUMA model generates fictive heating fields near the surface, which needs to be considered when analysing the results.

The meridional cross section of the zonally averaged forcing field (Fig. 1b) is comparable to the total diabatic heating composed of the net radiative heating, the latent heat release and boundary layer heating (see Peixoto and Oort 1992). The forcing field shows large positive values of about 3 K/day in the lower troposphere around 30°N and negative contributions of about -3 K/day at high latitudes related to the boundary layer heating. In the tropics the maximum mid-tropospheric heating of about 2 K/day is associated with the latent heat released by strong convective precipitation in the Inter Tropical Convergence Zone (ITCZ).

This PUMA forcing field leads to a time-mean climate, which is very similar to the ECHAM2/OPYC control climate. For example, Fig. 2 shows the wind field in 300 hPa for PUMA and the related ECHAM2/OPYC control field. Both models show the same intensities and locations of the winter jet streams, with

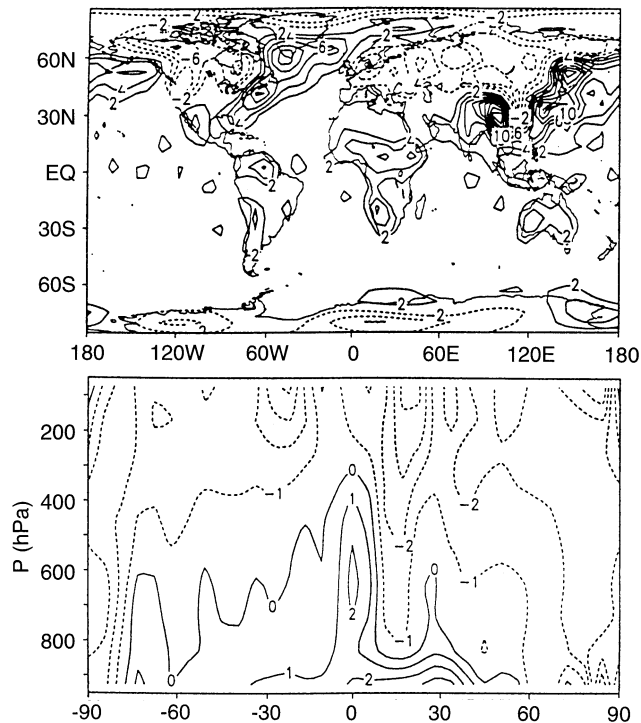


Fig. 1 Upper panel: Horizontal distribution of the heating at 950 hPa. Contours every 2 K/d. Lower panel: Vertical cross section of the zonally averaged heating. Contours every 0.5 K/d; negative contours are dashed

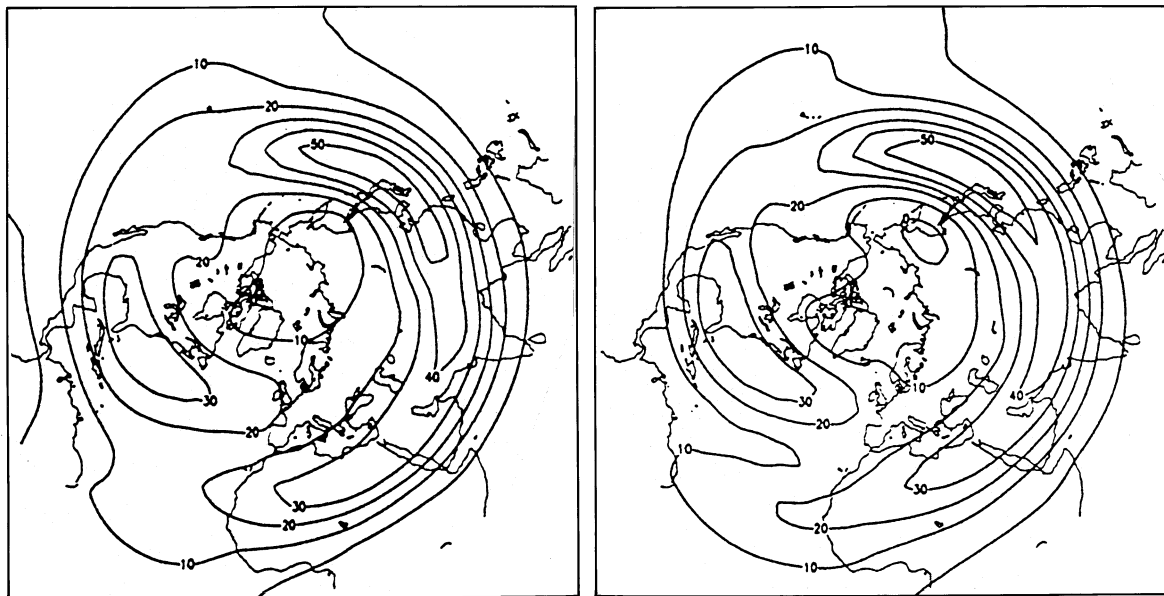


Fig. 2 Ten-year averaged 300 hPa zonal wind for the PUMA CTL run (left panel) and for the ECHAM2/OPYC CTL run (right panel). Contours every 10 m/s

50 m/s in the Pacific and 30 m/s in the Atlantic region. The main differences between the two models are found near the surface which is due to the highly simplified PUMA boundary conditions (for example, no land – sea contrast).

The ECHAM transient eddy features are reasonably well reproduced by PUMA. The bandpass filtered variance of the 500 hPa height field and the northward flux of sensible heat at 900 hPa of PUMA and ECHAM2/OPYC simulations are presented in Fig. 3. The fields show the time filtered 2.5 to 6 day variability (Blackmon 1976). The Atlantic storm track is correctly located, but the maximum intensity is underestimated.

The Pacific storm track is stronger and shifted upstream in the PUMA model. The meridional temperature flux at 900 hPa (Fig. 3 lower panel) shows maximum intensity located slightly south of the storm tracks. Compared with ECHAM, however, the PUMA simulation overestimates the temperature flux over the western Pacific by about 10 K m/s and underestimates the northward temperature transport at the western Atlantic by about 3 K m/s. These deviations may be attributed to the moist processes lacking in the PUMA model.

The correspondence between the PUMA and ECHAM2/OPYC scenario and control runs is of high quality. The average zonal-mean temperature

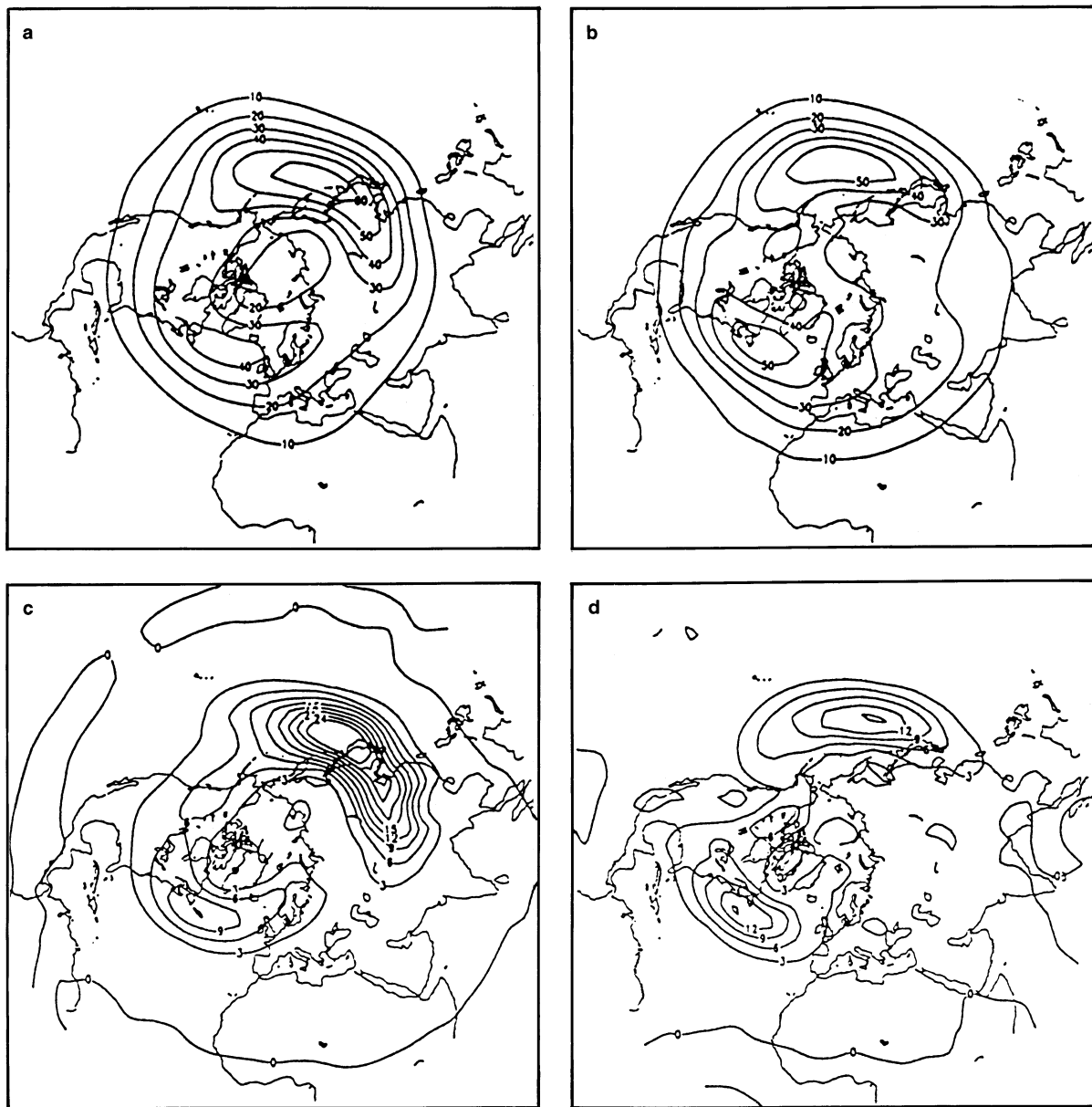


Fig. 3a–d Upper panel: bandpass filtered Northern Hemisphere 500 hPa geopotential height variance; **a** PUMA CTL run, **b** ECHAM2/OPYC CTL run. Contours every 10 gpm. Lower panel:

bandpass filtered Northern Hemisphere 900 hPa meridional temperature flux; **c** PUMA CTL run, **d** ECHAM2/OPYC CTL run. Contours every 3 K/m

difference between the PUMA SCE and CTL experiments is shown in Fig. 4. The climate change signal is clearly visible and shows all the features discussed, for example by Hall et al. (1994). These include a maximum greenhouse warming at low levels in higher latitudes, implying a weakening of low-level baroclinicity at mid-latitudes and a large greenhouse warming in the tropical upper troposphere with an associated increase in upper-tropospheric meridional temperature gradients. As in the ECHAM2/OPYC simulations the changes of the three dimensional time-mean state are related to storm track displacements with small magnitudes. The Atlantic storm track shows a downstream intensification and a weakening at the upstream end and at the centre (Fig. 5). The Pacific storm track is intensified at the upstream end and weakened downstream and in the centre.

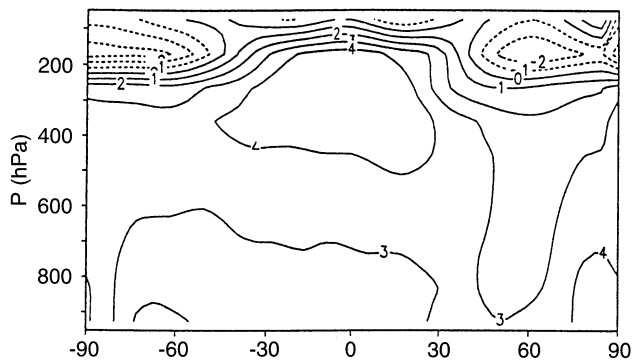


Fig. 4 Vertical cross section of the zonally averaged temperature difference between the scenario and the control simulation (SCE-CTL). Contours every 1 K

The transient eddy activity is related to the baroclinicity of the time-mean flow defined by the maximum Eady growth rate (Eady 1949; Lindzen and Farrell 1980) :

$$\sigma_{BI} = 0.31 \frac{f}{N} \frac{\partial |v|}{\partial p} = 0.31 \frac{1}{T} \left(\frac{1}{g\theta} \frac{\partial \theta}{\partial z} \right)^{-1/2} |\nabla T| \quad (6)$$

Figures 6a,b presents the difference between the maximum Eady growth rates (PUMA, SCE-CTL) integrated

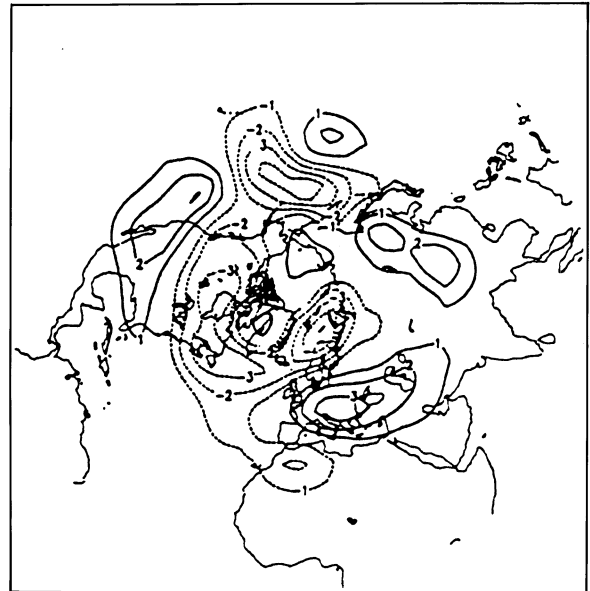


Fig. 5 Ten-year mean difference (SCE-CTL) of the bandpass filtered Northern Hemisphere 500 hPa geopotential height variance. Contours every 1 gpm

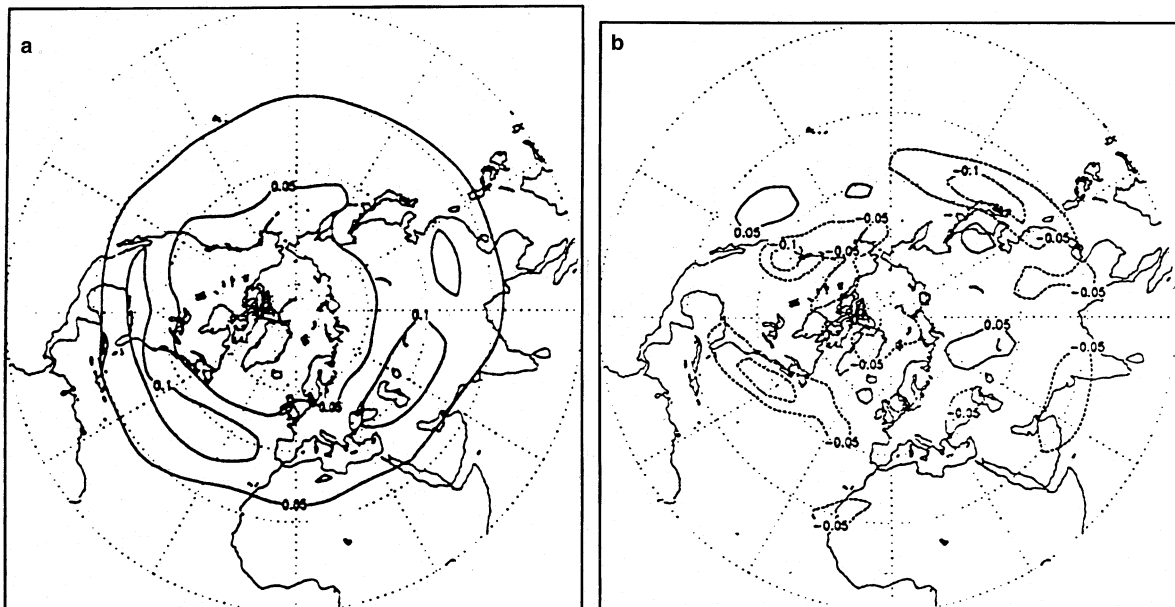


Fig. 6a, b Difference of the maximum Eady growth rate between the scenario and the control (SCE-CTL) for PUMA: **a** upper troposphere average (550–150 hPa) and **b** lower troposphere average (950–650 hPa). Contours every 0.05 d^{-1} . Negative contours are dashed

over the upper and over the lower troposphere, separately. The relationship between the storm track signal and the respective changes of the time-mean flow is not straight forward, because the Eady growth rates show opposing signs for the upper and lower troposphere: The upper-level baroclinicity increases everywhere in the PUMA SCE simulation with a maximum intensification of about 0.1 K/d (Fig. 6a). The changes in low-level baroclinicity (Fig. 6b) show a non-uniform structure. The baroclinicity decreases over the western Pacific and the Atlantic Oceans. The strongest amounts occur equatorwards to the upstream end of the storm tracks. In some areas further downstream the baroclinicity increases. Some of the low-level σ_{BI} -changes confirm the changes of the storm tracks discussed in Fig. 5, some show contradictory effects, for example over Europe.

This raises the question about the relationship between the maximum Eady growth rate, σ_{BI} , the storm track intensity, and the implications which the opposing changes in the upper- and the lower-level baroclinicity have on the transient eddy activity. This problem is addressed in the following section by employing PUMA sensitivity experiments.

5 Sensitivity experiments: baroclinicity and eddy activity

The sensitivity experiments focus on changes of eddy activity resulting from greenhouse warming and concentrates on the robustness of the predicted changes and their relation to the time mean flow. They are motivated by the results from the SCE simulation (Sect. 4), which show an inhomogeneous three-dimensional structure of the response. In particular, the predicted changes of upper- and lower-level baroclinicity suggest opposing effects on the eddy activity.

Considering the Eady model as the most simple representation of the baroclinic troposphere, where the baroclinic instability is realised by a uniform meridional temperature gradient, upper- and lower-level baroclinicity appear to be equally important. However, using a more comprehensive three-layer quasi-geostrophic β -channel model, which is horizontally homogeneous, Held and O'Brien (1992) conclude that eddy fluxes and energies are larger when the shear is concentrated at lower than at higher levels, so that the eddy flux activity is more sensitive to changes of the lower- than to the upper-level meridional temperature gradients. This is supported by Pavan (1996) analysing the sensitivity of the mid-latitude tropospheric eddies to changes of the meridional temperature gradient due to CO₂ doubling. Pavan (1996) shows that a dry multi-level quasi-geostrophic model is much more sensitive to the lower than to the upper tropospheric temperature gradient. Therefore, in a enhanced CO₂ scenario climate the effects of the decrease in the lower tropo-

spheric meridional temperature gradient should dominate the response while increasing the upper tropospheric gradient should have only a minor influence on the climatology. However, these models are rather simple and do not consider the full three-dimensional structure of the circulation.

In two sets of PUMA sensitivity studies we extend the idealised experiments of Held and O'Brien (1992) and Pavan (1996) to more realistic conditions. In particular, two important features are taken into account: the organisation of Northern Hemisphere eddy activity into the North Atlantic and North Pacific storm track and the pronounced three-dimensional structure of the temperature response in the greenhouse warming scenario. The sensitivity experiments are based on the result of the PUMA SCE simulation. In one set (a) the sensitivity of the storm tracks to changes of lower- and upper-level zonal mean baroclinicity is analysed. In the second set (b) the effects of the full three-dimensional temperature response on the eddy activity is investigated.

5.1 Zonal mean sensitivity experiments

PUMA sensitivity experiments can be simply realised by a restoration temperature that is assimilated by a modified target temperature. To separate the upper- and lower-level effects on the mid-latitude eddy activity, only the lowest model layers (about 950–550 hPa) are modified by amplifying and reducing the zonal-mean gradient of the target temperature. Changes of the SCE temperature gradient by $\pm 10\%$, $\pm 20\%$, $\pm 30\%$ and $\pm 50\%$ are tested in individual experiments. Likewise the influence of the upper-level temperature gradient (about 550–150 hPa) is tested. These 16 sensitivity experiments (referred to as SEN) relative to the SCE scenario climate are integrated for 100 y, where the last 10 y are subjected to analysis. The following results are noted.

Figure 7 shows the bandpass filtered variance of the 500 hPa geopotential height field for the Northern Hemisphere as the difference SEN-SCE. Results are presented for the four most extreme experiments: upper level amplification by 50% (Fig. 7a), upper level reduction by 50% (Fig. 7b), lower level amplification by 50% (Fig. 7c) and lower level reduction by 50% (Fig. 7d). In general, the results confirm the idealised experiments by Held and O'Brien (1992) and Pavan (1996). An overall increase of eddy activity is observed with enhanced baroclinicity and vice versa, while the sensitivity to lower-level modifications are significantly larger. This result is summarised in Fig. 8, where the Northern Hemisphere average of the bandpass filtered geopotential height variance is plotted as a function of the global average of the low-level (solid line) and upper-level (dotted line) σ_{BI} variation using all 16 sensitivity simulations. Both curves show a nearly linear dependence,

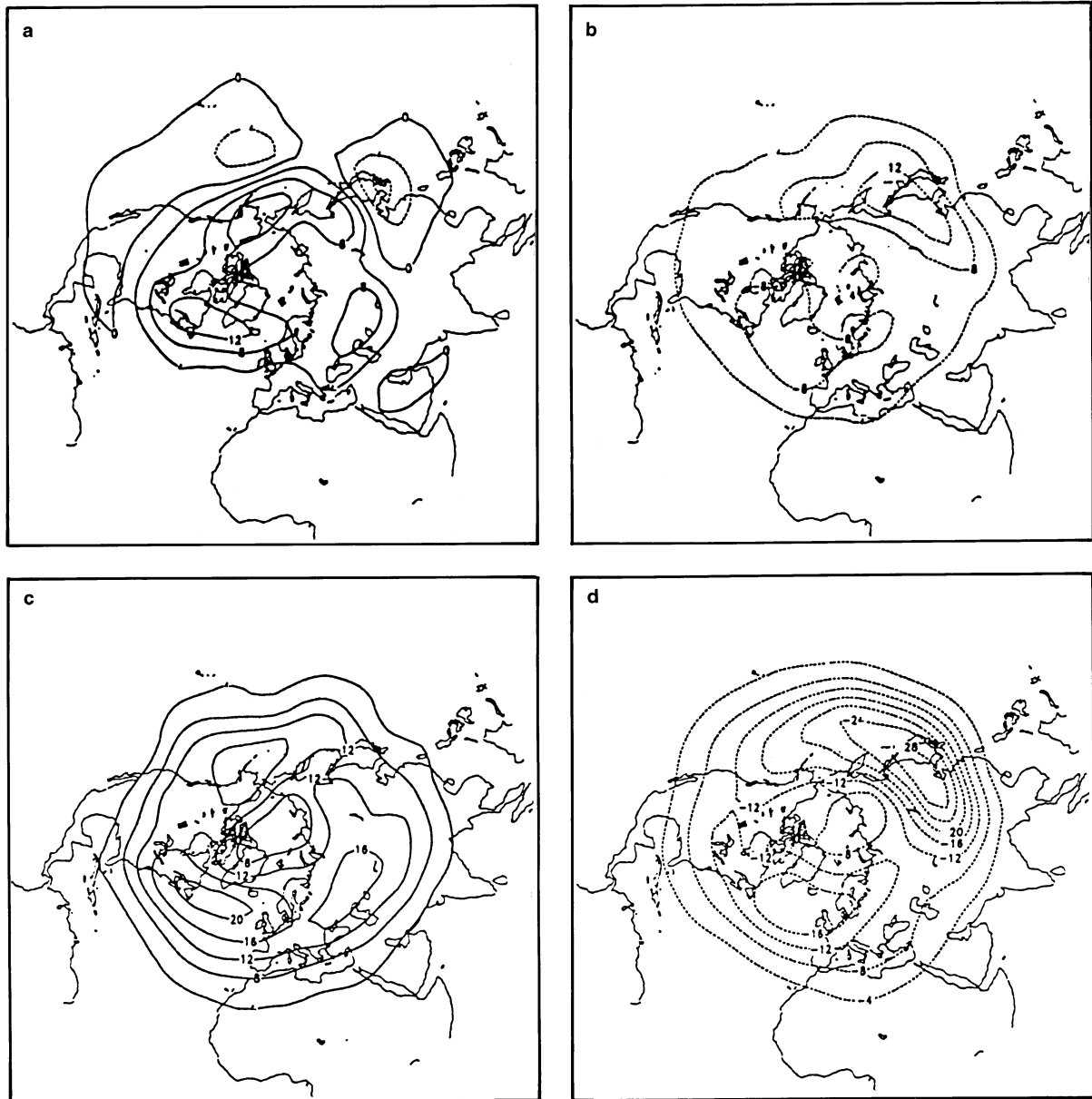


Fig. 7a–d Differences (SEN-SCE) of the bandpass filtered Northern Hemisphere 500 hPa variance for the zonal-mean sensitivity experiments: **a** upper-level amplification by 50%, **b** upper-level reduction

by 50%, **c** low-level amplification by 50%, **d** low-level reduction by 50%. Contours every 4 gpm

while the slope of the low level intensification is about twice as steep as the upper-level intensification. These results are supported also by other eddy characteristics, such as the poleward momentum- and temperature flux or the transient eddy kinetic energy (not shown).

A more careful inspection of Fig. 7 shows different behaviour for the North Atlantic and the North Pacific storm track. For all simulations, the response of the North Atlantic storm track is an entire strengthening or weakening, whereas the anomalies have the same shape as the storm track itself (see Fig. 3). This is not the case for the North Pacific storm track. Here, the

increase of baroclinicity has only minor impact on the strength of the storm track and results only in a slight northeastward shift. The decrease of baroclinicity, on the other hand, leads to a weakening of the upstream end of the Pacific storm track. Our results are, to some extent, in harmony with an observational study by Nakamura (1992), in particular the difference of the North Atlantic and North Pacific storm track anomalies, which are unexpected from the idealised experiments by Held and O'Brien (1992) and Pavan (1996). Nakamura (1992) investigated the North Atlantic and North Pacific eddy activity based on about 20 y

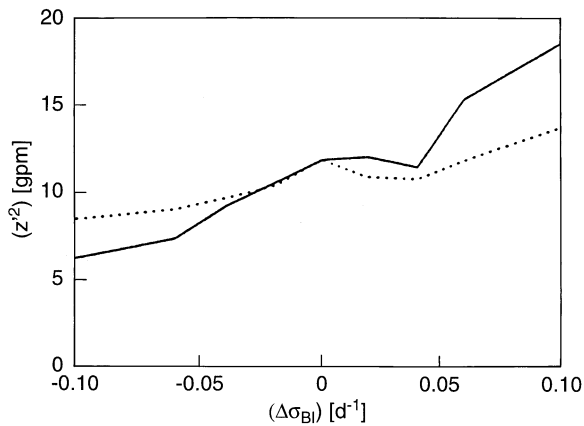


Fig. 8 Northern Hemisphere average of the bandpass filtered 500 hPa geopotential height variance (units: gpm) as function of low-level (*solid line*) and upper-level (*dotted line*) Eady growth rate change (units: d^{-1})

of data. For the North Atlantic he found a single maximum of baroclinic wave activity in January, consistent with a maximum of baroclinicity during this period. For the North Pacific, however, the eddy activity exhibits two peaks in late autumn and in early spring and a significant weakening in midwinter despite the fact that the baroclinicity and the intensity of the Pacific jet are strongest in midwinter. Nakamura (1992) relates his findings to the suppression of the growth of baroclinic wave by the strong jet stream generated by the larger temperature gradients. Up to a maximum wind speed of about 45 m/s, the eddy activity increases with increasing baroclinicity, while beyond this value a decrease of eddy activity is observed.

5.2 Three-dimensional sensitivity experiments

For the three-dimensional sensitivity study, the target temperature is modified using the temperature difference between the SCE and CTL simulation. As for the zonal mean experiment, the atmosphere is divided into a lower part (about 950–550 hPa) and an upper part (about 550–150 hPa). The target temperatures for the individual sensitivity simulations are modified in order to amplify or weaken the upper- or lower-level baroclinicity by the SCE-CTL response pattern (Fig. 6) of different size. Eight simulations are performed, where the baroclinicity of the respective levels is varied by $\pm 50\%$ and $\pm 100\%$ the SCE-CTL response. Note, that a reduction by 100% is similar to CTL conditions. These eight sensitivity experiments (SEN) relative to the scenario climate (SCE) are integrated for 100 y, where the last 10 y are subjected to analysis.

Figure 9 presents the response (SEN-SCE) of the bandpass filtered variance of the 500 hPa height field for the four most extreme: (a) change of the upper-level baroclinicity by $+1 \times$ (SCE-CTL), (b) change of the

upper-level baroclinicity by $-1 \times$ (SCE-CTL), (c) change of the lower-level baroclinicity by $+1 \times$ (SCE-CTL) and (d) change of the lower-level baroclinicity by $-1 \times$ (SCE-CTL). The response differs significantly for all simulations and indicates the level of uncertainty of the SCE-CTL eddy activity response, if we consider all the uncertainties of the change of the temperature distribution due to the greenhouse warming.

The common mean characteristics of the sensitivity to the upper- and lower-level baroclinicity change are calculated by averaging the variance anomalies of the respective four SEN simulations weighted by the magnitude of the σ_{BI} -change. The results are displayed in Fig. 10. Considering the modification of the baroclinicity in the individual simulations, the results are unexpected. Eddy activity enhances while baroclinicity weakens and vice versa, which already appears in Fig. 9. The dominant response to the SCE-CTL upper-level change, which is a general increase of baroclinicity (see Fig. 6a), is a decrease of eddy activity in the Pacific sector. The maximum decrease is located north of the Pacific storm track and extends up- and downstream over the continents. Also, the Atlantic storm track is weakened at its northern flank. An increase of eddy activity is found over central Europe. For the lower-level σ_{BI} changes according to the SCE-CTL results (dominated by a reduction of baroclinicity; Fig. 6b), we find enhanced eddy activity, especially over the western Oceans and Asia and a weak decrease of eddy activity in the northern North Atlantic sector.

A possible explanation for the unexpected response can be obtained from a theoretical study by Pierrehumbert (1984). In an idealised framework, Pierrehumbert (1984) shows that flows with localised baroclinicity can support two classes of unstable modes, local and global, with the local modes having their maximum amplitude downstream of the maximum baroclinicity. The growth rate of the local modes are determined locally at the point of maximum baroclinicity. The growth rates of the global modes, on the other hand, are determined by the averaged baroclinicity over the domain. It takes a longer time for global than for local modes to emerge from random initial conditions. In contrast to the conventional local maximum growth rate, the growth rate of the local modes decreases with increasing vertically averaged flow. In order to obtain local modes, the ratio of maximum baroclinicity and minimum baroclinicity downstream of the maximum must be sufficient large.

Our results may be related to Pierrehumbert's (1984) findings as follows: if we compare the changes of low-level baroclinicity (Fig. 6b) with the vertical average of the baroclinicity itself (Fig. 11), their reduction is located at the downstream end of both σ_{BI} maxima, while the maxima themselves remain unchanged. This leads to a sharpening of the baroclinicity peaks and, with respect to Pierrehumbert's (1984) results, makes the growth of local modes more likely. In addition, the

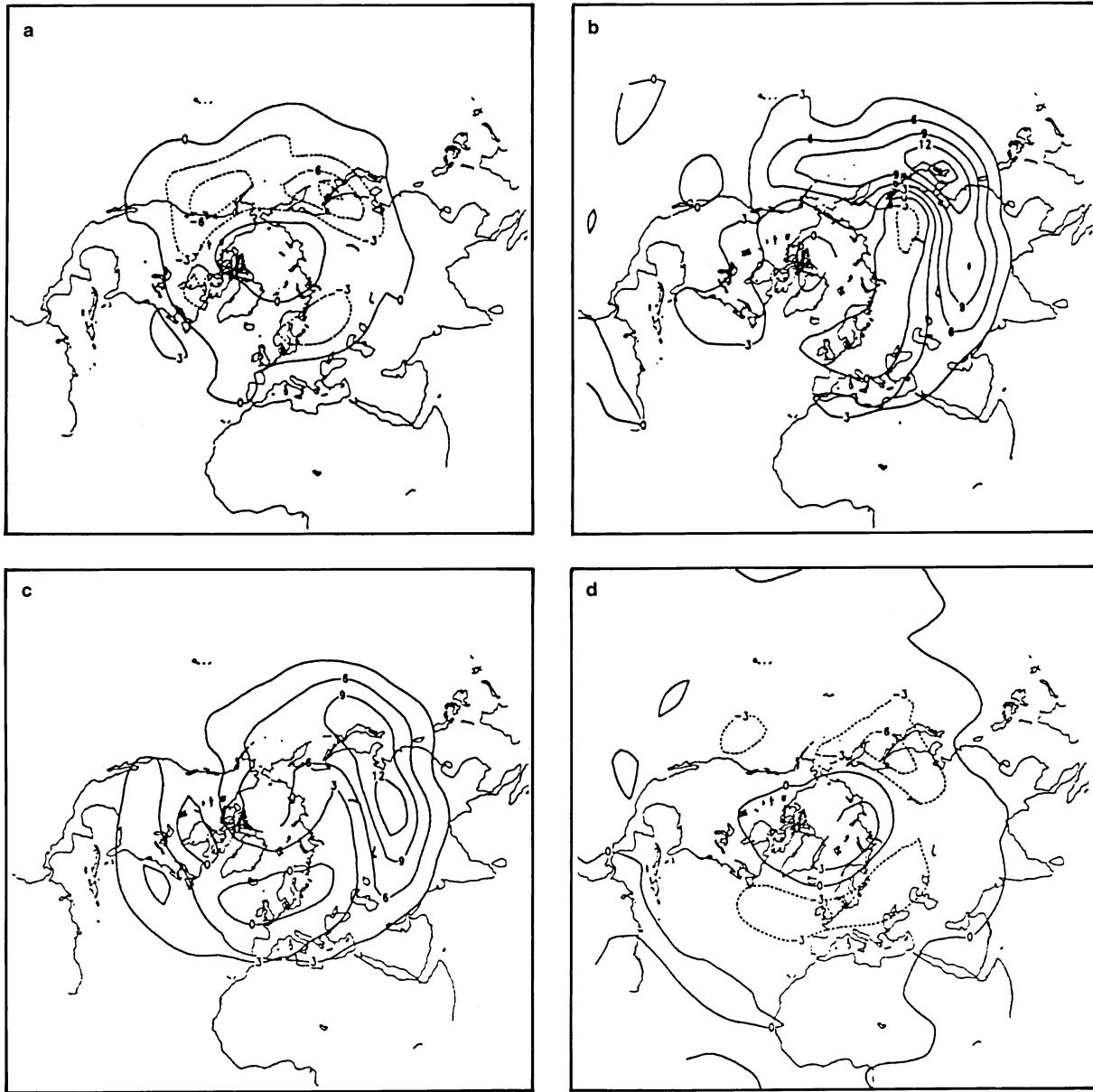


Fig. 9a–d Difference (SEN-SCE) of the bandpass filtered Northern Hemisphere 500 hPa geopotential height variance for the three-dimensional sensitivity experiments: **a** upper-level amplification by

100%, **b** upper-level reduction by 100%, **c** low-level amplification by 100%, **d** low-level reduction by 100%. Contours every 3 gpm

strengths of jet streams decrease slightly due to the overall decrease of the temperature gradient (not shown). Both effects can contribute to the observed enhancement of eddy activity (Fig. 10b), if we assume that the observed eddy activity is dominated by local modes.

The upper level baroclinicity change (Fig. 6a) exhibits an increase with a large zonally symmetric component, leading to a strengthening of both jets. Relative maxima are located over the North Atlantic and the Eurasian continent. The latter reduces the baroclinicity gradient upstream of the North Pacific storm track. This effect is supported by the relative minimum of the

baroclinicity change close to the maximum of σ_{BI} . Referring again to the local mode argument, both the increase of the jet and the decrease of the baroclinicity gradient correspond to the observed decrease of eddy activity in the Pacific. The same arguments hold for the Atlantic sector, where the relative maximum of baroclinicity change is located downstream of the σ_{BI} maximum. In addition, the maximum of baroclinicity change over the North Atlantic supports the increase of eddy activity, which occurs over Europe. This increase downstream of the North Atlantic storm track, on the other hand, is already present in the zonal mean experiment and may also be a consequence of the

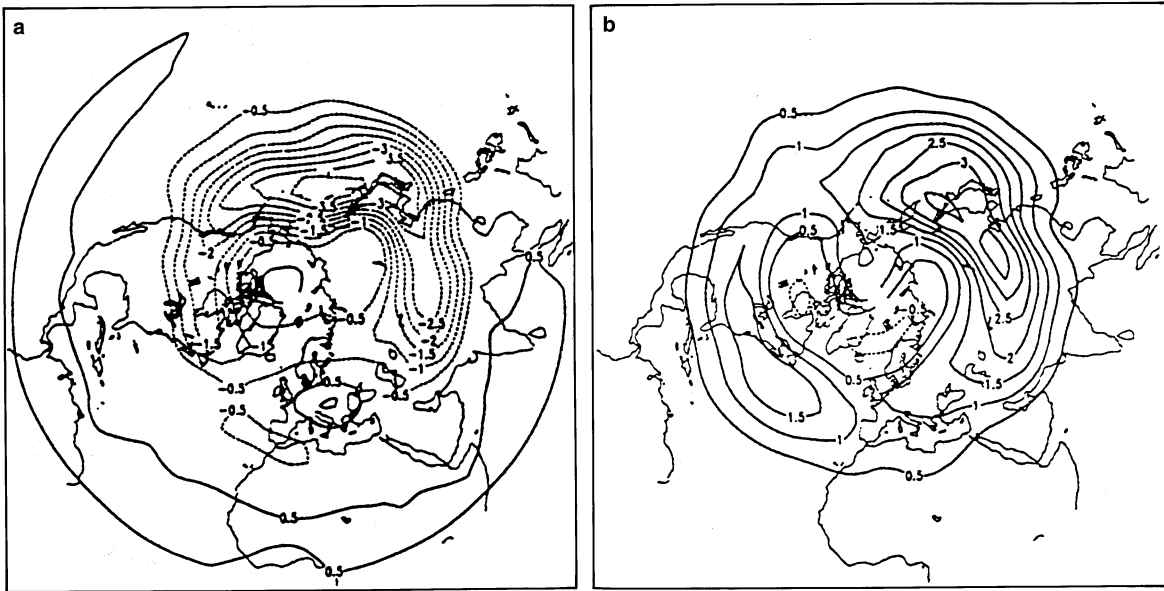


Fig. 10 **a** Upper-level and **b** lower-level response of the 500 hPa geopotential height variance obtained by combining all upper- and lower-level patterns scaled by their respective temperature change. Contours every 0.5 gpm

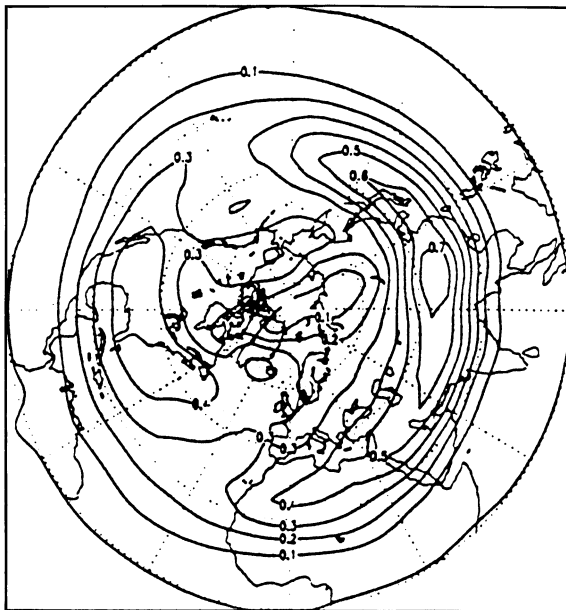


Fig. 11 Vertically averaged (950–150 hPa) maximum Eady growth rate for the PUMA SCE simulation. Contours every 0.1 d^{-1}



Fig. 12 Linear combination of the upper-level and lower-level storm track response (Fig. 10). Contours every 1 gpm

enhanced advection of eddies by the enhanced time-mean flow.

In summary, large parts of the response of the eddy activity in the sensitivity simulations can be explained by the respective changes of the baroclinicity distribution. The results are consistent with the assumption that the changes of eddy activity are dominated by local modes of baroclinic instability as proposed by Pierrehumbert (1984). In particular, these local modes

can explain an increase of eddy activity with decreasing overall baroclinicity, which is unexpected from the classical Eady view and the studies by Held and O'Brien (1992) and Pavan (1996). However, the large spectrum of the responses in the different sensitivity simulations, as presented in Fig. 9, leads to the question, to what extent can the total SCE-CTL response be related to the individual upper- or lower-level changes? This is answered by Fig. 12, presenting the linear combination

(upper-level plus lower-level) of the responses (Fig. 10a,b). A large part of the response to changes of baroclinicity of the upper- or lower-level baroclinicity is cancelled out by opposing response to the changes in the other level. The main features of the SCE-CTL response are reproduced by the remaining anomalies (see Fig. 5) indicating that the basic relationships between the individual changes of baroclinicity and the eddy activity, as analysed in the sensitivity simulations, are relevant for the total SCE-CTL response. In particular, the relevance of the pronounced three-dimensional structure of both, the eddy activity (organised as storm tracks) and the response of the mean flow due to the increase of CO_2 , for the results is pointed out.

5.3 Robustness of the sensitivity experiments: implications of orography

The results of the assimilation runs indicate that the target climate can be reproduced largely by treating its temperature distribution only. This suggests that the temperature fields, and thus the height fields, contain sufficient information so that the degrees of freedom for choosing an appropriate restoration temperature distribution are large enough to incorporate the required forcing. However, it can be shown that the assimilation technique proposed here is unsuccessful in the framework of a linearised quasi-geostrophic two-level model with orography. In such a simple two-level model there are two degrees of freedom, the barotropic and the baroclinic mode, defining the climate. While both modes are forced by orography, only one, the baroclinic, can be forced by heating.

Therefore, the influence of orographic effects on our PUMA-experiments needs to be tested. This is performed by a set of additional assimilation runs adopting an ECHAM-like orography for PUMA. The results are summarised as follows:

1. In general, the quality of reproducing the ECHAM target climate with respect to the mean flow or the transient variability is not improved significantly by including orography. In particular, discrepancies of some eddy characteristics, for example the transport of sensible heat by transient eddies (Fig. 3), are not diminished. The shortcomings of the PUMA assimilation can therefore be related to other features (than orography) as, for example, the lack of moisture and thus latent heat release. That is, the present Newtonian cooling formulation does not allow different heating time scales; it always dampens temperature anomalies, which contrasts the rapid heating rates required for latent heat release.
2. The results with orography are more sensitive to changes of external model parameters such as the time scales for Newtonian cooling and Rayleigh friction, or the horizontal hyperdiffusion. These external parameters are to a large extent artificially

chosen. Thus, more tuning is needed to obtain a setup to ensure a sufficient agreement between PUMA and the target climates. The enhanced sensitivity is unexpected. It may be speculated that orography adds more degrees of freedom to the PUMA climate, which therefore becomes less stable to variations of external forcing.

There is, of course, no doubt that orography is an important factor for the behaviour of the atmospheric circulation. The aim of the present study, however, is to demonstrate a possible way for using simplified circulation models to analyse GCM (or observational) results. The study focus on the sensitivity of the storm tracks to changes of mean flow baroclinicity. The omission of orography might, in this respect, be seen as a strong, but tolerable, further simplification of the already simplified global circulation model PUMA. In the framework of using simplified models, simplifications appear to be valid, if the results prove to be sufficiently reliable for the problem under consideration.

The robustness analysis shows that neglecting the orography is appropriate for the present study investigating the effect of changes in baroclinicity. Other applications, however, may require orography together with an improved choice of (a) the assimilation time scale and (b) the parametrisation of hyperdiffusion. The appropriate experiments have been performed and show the following results: (a) a much longer integration time is needed to approach a quasi-stationary state if the time scale for the restoration temperature update (τ_A) is the same as in the simulations without orography. In order to reach the quasi-stationary state in a reasonable time, it is necessary to use a much smaller τ_A (approximately 5 days) than without orography. This shorter time scale enhances variability of the restoration temperature during the update, but the time averaged T_E distribution and the final climate remain almost unaffected. (b) The eddy activity is considerably reduced using the simple ∇^8 horizontal diffusion scheme. Synoptic variability within the ECHAM-range is obtained, however, by changing the horizontal diffusion scheme to the ECHAM formulation, which is a ∇^2 damping for waves with wave numbers larger than 15 (Roeckner et al. 1992; Laursen and Eliassen 1989). The results without orography are not significantly affected by the individual choice of the horizontal diffusion.

6 Conclusion

Here we investigate the influence of upper and lower tropospheric changes, due to the greenhouse warming effect, on the Northern Hemisphere winter storm tracks. A simplified global circulation model (PUMA) is used to analyse a warmer CO_2 climate scenario simulated by a global coupled atmosphere-ocean general circulation

model, GCM. In order to represent the prescribed GCM climates by PUMA, restoration temperature fields are assimilated by a dynamical relaxation towards a three-dimensional time-mean temperature distribution adopted from GCM experiments (control and scenario). This leads PUMA to simulate the GCM time-mean and eddy characteristics with reasonable accuracy: Both models show a downstream intensification of the Atlantic storm track, and a displacement of the Pacific storm track due to the greenhouse warming effect.

The influence of the opposing baroclinicity changes in the upper and lower troposphere is analysed by two sets of sensitivity studies. One set analyses the response of eddy activity to changes in zonal mean baroclinicity, by varying the meridional temperature gradient in the upper and lower troposphere of the scenario climate, respectively. The second study analyses the impact of baroclinicity changes, due to the global warming, on the transient eddy activity by considering the three-dimensional structure of the temperature changes. Again the scenario climate is varied in the upper and lower troposphere. The following results of the sensitivity studies are noted:

6.1 Zonal mean sensitivity experiment

1. In general, the eddy activity increases with increasing zonal-mean baroclinicity and vice versa. The eddy activity is more sensitive to lower- than to upper-level baroclinicity changes confirming the results from quasi-geostrophic β -channel models by Held and O'Brien (1992) and Pavan (1996).
2. Different responses emerge for the North Atlantic and the North Pacific storm track. While the entire North Atlantic storm track is enhanced (weakened) due to an increase (decrease) of baroclinicity, the North Pacific storm track is not much effected by an increase of baroclinicity, but shows a weakening with decreasing baroclinicity. These results are, to some extent, in harmony with an observational study by Nakamura (1992), and might be related to a suppression of the growth of baroclinic waves by a jet stream exceeding a certain strength.

6.2 Three-dimensional sensitivity experiment

1. The three-dimensional sensitivity study does not confirm the simple correlation between baroclinicity and eddy activity suggested by the idealised studies. The eddy activity in the PUMA simulation is more sensitive to the local distribution of baroclinicity than to its zonal average. Stronger local gradients in baroclinicity are related to enhanced eddy activity and vice versa.
2. The results suggest that the eddy activity in the PUMA simulation is dominated by local modes of

baroclinic instability proposed by Pierrehumbert (1984).

3. A large part of the eddy response can be consistently attributed to the opposing effects of upper- and lower-level baroclinicity changes on the local modes of baroclinic instability.
4. In order to analyse the global warming effect on the mid-latitude storm tracks the three-dimensional structure of the atmospheric changes need to be considered.

Considering all the important feedbacks, sensitivity studies must be performed by complex GCMs. However, these experiments are difficult to realise because of their demand on computer time. In addition, the complex structure of the GCM and the large number of feedback mechanisms makes the design of sensitivity experiments difficult. The present study shows that simplified general circulation models are a useful and practically applicable alternative to perform sensitivity studies on the dynamical interpretation of climate experiments. PUMA, for example, requires only a fraction of the computing time of a full GCM and still allows a reasonable representation of the global circulation. Employing the assimilation technique proposed here, the prescribed climate can be reproduced surprisingly well so that numerical sensitivity experiments can be almost ideally performed by PUMA-type models. In this way, the simplified PUMA model has proven to be a useful additional tool for analysing GCM dynamics, and it may also be useful for further investigations, for example, to study the sensitivity of GCM simulations to polar-ice distributions or sea-surface temperatures, etc. However, the simplifications contained in the PUMA model, for example neglecting moist processes and using simplified boundary conditions, need to be considered when discussing the results.

Acknowledgements We thank J. Egger and another reviewer for their helpful comments and suggestions. We acknowledge the financial support provided by the Bundesministerium für Bildung, Wissenschaft, Forschung und Technologie (07VKV01/1), the ARC-project (313-ARC-IX-scu) and the European Community under contract EV5V-CT94-0503.

References

- Blackmon ML (1976) A climatological spectral study of the 500-mb geopotential height of the Northern Hemisphere. *J Atmos Sci* 33: 1607–1623
- Blackmon ML, Wallace JM, Lau NC, Mullen SL (1977) An observational study of the Northern Hemisphere wintertime circulation. *J Atmos Sci* 34: 1040–1053
- Charney J (1947) The dynamics of long waves in a baroclinic westerly current. *J Meteorol* 4: 35–63
- Eady ET (1949) Long waves and cyclone waves. *Tellus* 1: 33–52
- Frisius T, Lunkeit F, Fraedrich K, James IN (1998) Storm-track organization and variability in a simplified atmospheric global circulation model. *Q J R Meteorol Soc* 124: 1019–1043
- Hall NMJ, Hoskins BJ, Valdes PJ, Senior CA (1994) Storm tracks in a high-resolution GCM with doubled carbon dioxide. *Q J R Meteorol Soc* 120: 1209–1230

- Held IM, O'Brien E (1992) Quasigeostrophic turbulence in a three-layer model: effect of vertical structure in the mean shear. *J Atmos Sci* 49: 1861–1870
- Hoskins BJ, Simmons AJ (1975) A multi-layer spectral model and the semi-implicit method. *Q J R Meteorol Soc* 101: 637–655
- James IN, Gray LJ (1986) Concerning the effect of surface drag on the circulation of a planetary atmosphere. *Q J R Meteorol Soc* 112: 1231–1250
- James IN, James PM (1992) Spatial structure of ultra-low-frequency variability of the flow in a simple atmospheric circulation model. *Q J R Meteorol Soc* 118: 1211–1233
- James PM, Fraedrich K, James IN (1994) Wave-zonal-flow interaction and ultra-low-frequency variability in a simple atmospheric circulation model. *Q J R Meteorol Soc* 120: 1045–1067
- Laursen L, Eliassen E (1989) On the effects of the damping mechanisms in an general circulation model. *Tellus* 41A: 385–400
- Lindzen RS, Farrell B (1980) A simple approximate result for the maximum growth rate of baroclinic instabilities. *J Atmos Sci* 37: 1648–1654
- Lunkeit F, Sausen R, Oberhuber JM (1996a) Climate simulations with the global coupled atmosphere-ocean model ECHAM2/OPYC. Part I: Present-day climate and ENSO events. *Clim Dyn* 12: 195–212
- Lunkeit F, Ponater M, Sausen R, Sogalla M, Ulbrich U, Windelband M (1996b) Cyclonic activity in a warmer climate. *Contrib Phys Atmos* 69: 353–407
- Mole N, James IN (1990) Baroclinic adjustment in a zonally varying flow. *Q J R Meteorol Soc* 116: 247–268
- Nakamura H (1992) Midwinter suppression of baroclinic wave activity in the Pacific. *J Atmos Sci* 49: 1625–1870
- Oberhuber JM (1993a) Simulation of the Atlantic circulation with a coupled sea-ice-mixed layer-isopycnal general circulation model. Part I: Model description. *J Phys Oceanogr* 23: 808–829
- Oberhuber JM (1993b) Simulation of the Atlantic circulation with a coupled sea-ice-mixed layer-isopycnal general circulation model. Part II: Model experiment. *J Phys Oceanogr* 23: 830–845
- Pavan V (1996) Sensitivity of a multi-layer quasi-geostrophic β -channel to the vertical structure of the equilibrium meridional temperature gradient. *Q J R Meteorol Soc* 122: 55–72
- Peixoto JP, Oort AH (1992) *Physics of climate*. American Physical Society (New York) 520p
- Phillips NA (1951) A simple three-dimensional model for the study of large-scale extratropical flow patterns. *J Meteorol* 8: 381–394
- Pierrehumbert RT (1984) Local and global baroclinic instability of zonally varying flow. *J Atmos Sci* 41: 2141–2162
- Roeckner E, Arpe K, Bengtsson L, Brinkop S, Dümenil L, Esch M, Kirk E, Lunkeit F, Ponater M, Rockel B, Sausen R, Schlese U, Schubert S, Windelband M (1992) Simulation of the present-day climate with the ECHAM model: impact of model physics and resolution. Max-Planck-Institut für Meteorologie, Rep 93, Hamburg, FRG
- Siegmund PC (1990a) Linear simulation of the stationary eddy response of a general circulation model to a doubling of atmospheric CO₂. *KNMI Sci Rep*
- Siegmund PC (1990b) The effect of a doubling of atmospheric CO₂ on the storm tracks in the climate of a general circulation model. *KNMI Sci Rep*, WR 90-01
- Stephenson DB, Held IM (1993) GCM response of northern winter stationary waves and storm tracks to increasing amounts of carbon dioxide. *J Clim* 6: 1859–1870
- von Storch H, Guddal J, Iden KA, Jónsson T, Perlwitz J, Reistad M, De Ronde J, Schmidt H, Zorita E (1993) Changing statistics of storms in the North Atlantic? Max-Planck-Institut für Meteorologie, Report 116, Hamburg, FRG
- Valdes JP, Hoskins BI (1989) Linear stationary wave simulations of the time-mean climatological flow. *J Atmos Sci* 46: 2509–2527